Publ. Astron. Soc. Japan **41**, 1073–1082 (1989)

Structure of a Bright-Rimmed Globule in IC 1396*

Makoto NAKANO

Department of Earth Science, Faculty of Education, Oita University, Oita 870-11

Yoshio TOMITA and Hiroshi OHTANI

Department of Astronomy, Faculty of Science, Kyoto University, Sakyo-ku, Kyoto 606

Katsuo OGURA

Kokugakuin University, Higashi, Shibuya-ku, Tokyo 150

and

Yoshiaki SOFUE

Institute of Astronomy, The University of Tokyo, Mitaka, Tokyo 181

(Received 1989 February 27; accepted 1989 June 2)

Abstract

A bright-rimmed globule in IC 1396 has been observed in the ^{12}CO and ^{13}CO ($J=1$–0) lines with high spatial resolution using the 45-m telescope at the Nobeyama Radio Observatory. It has been found that the CO column density peaks at 0.1 pc inside the bright rim in the east. The central part of the globule, where two emission-line pre-main sequence stars (LkHα 349 and LkHα 349/c) exist, coincides with a CO cavity 0.4 pc in size. The CO structure is well correlated with the appearance of faint stars and nebulosities around the two stars. We suggest that the cavity is formed as a result of an interaction between the stellar wind from the pre-main sequence stars and the globule.

Key words: Globule; H II region; Molecules; Pre-main sequence.

1. Introduction

IC 1396 is a diffuse ring-like H II region 2°.5 in diameter associated with a small cluster called Trumpler 37. At the western part of the H II region, there is a prominent cometary globule named "comet tail No. 6" (Osterbrock 1957). This globule is outlined by a bright rim (Pottasch 1956) called "IC 1396A". Osterbrock (1957) noticed a relatively

* Based on observations made at the Nobeyama Radio Observatory (NRO). NRO is a branch of the National Astronomical Observatory, an inter-university research institute operated by the Ministry of Education, Science, and Culture.

high density of ionized gas in the rim. Near the center of this globule, Dibai and Esipov (1968) found a nebulous Hα emission-line star. This star was catalogued as an Orion population star LkHα 349 (HRC 308n) by Herbig and Rao (1972). Another emission-line star, LkHα 349/c, was found by Cohen and Kuhi (1979) at 17″ northwest of LkHα 349.

The first molecular line observations of this globule were made by Loren et al. (1975). They showed that the ^{12}CO and ^{13}CO ($J=1$–0) intensities are well correlated with the optical morphology of the globule, and suggested that there is a heating source within it. However, the spatial resolution of their observations was too low (2′.6) to show the internal structure of the globule. Later Wootten et al. (1983) made a cross mapping of 30″ resolution (centered on the globule center) in the ^{12}CO and ^{13}CO $J=2$–1 transition. The most remarkable feature of their profiles is a dip in the ^{13}CO column density near the stars.

In the present work we studied the structure of this remarkable cometary globule and, in particular, examined the density dip around the stars by ^{12}CO and ^{13}CO mapping at higher resolution.

2. Observations

2.1. *CO Observations*

Observations of the $J=1$–0 lines of ^{12}CO and ^{13}CO were carried out in January and June 1986 using the 45-m millimeter-wave telescope at the Nobeyama Radio Observatory (NRO). The half-power beam width of the telescope was 17″ at 115 GHz, corresponding to a linear size of 0.05 pc for an assumed distance of 750 pc (Matthews 1979). A 20-K cooled receiver with a Schottky barrier diode mixer with a single side band was employed, providing a system temperature of $T_{sys}=600$–1000 K. Data were collected by an acousto-optical spectrometer with 2048 channels of 37-kHz resolution. This corresponds to a velocity resolution of 0.1 km s^{-1} at 115 GHz. The efficiency of the main beam and aperture of the antenna at 115 GHz was about 0.3 and 0.25, respectively. The mapping center was taken at the position of LkHα 349: R. A. $=21^h35^m18^s.3$, Decl. $=+57°17'42''$ (1950.0). This coordinate was derived on the Palomar Sky Survey print using an X-Y measuring machine at the Kiso Observatory, and should be as accurate as 1″ or better. The telescope was operated in the position-switching mode. The reference position was chosen to be 20′ southeast of the mapping center. The calibration of the data was accomplished by referring to an ambient-temperature absorber in front of the receiver. The intensities of the ^{12}CO and ^{13}CO lines were then scaled to the radiation temperature T_R, those measured toward S140 IRS1 with the same telescope by Hayashi et al. (1987). We assumed $T_R(^{12}\mathrm{CO})=29$ K and $T_R(^{13}\mathrm{CO})=17$ K at S140 IRS1. The pointing accuracy was checked by measuring the 43-GHz SiO maser line of T Cep, and was confirmed to be within 10″. The mapped area is about 2′.5 × 2′.5 in ^{12}CO and 1′.5 (NS) × 3′ (EW) in ^{13}CO.

2.2. *Spectroscopic Observations*

Low-dispersion spectra have been obtained for the nebulosity associated with LkHα 349/c by using the 188-cm reflector at the Okayama Astrophysical Observatory. Two spectrograms (hypersensitized IIaO plate) were taken with the Cassegrain spectrograph

equipped with an image intensifier. A wavelength range of 3700–6800Å was covered with a reciprocal dispersion of 230Å mm^{-1}. The slit was oriented in the north-south direction through LkHα 349/c in order to cover the bright part of the nebulosity. The spectrogram was scanned with a PDS microdensitometer, and reduction was carried out with the spectrum-processing system SPECTRA at the Kiso Observatory.

3. Results

3.1. *Carbon Monoxide*

Figure 1 shows a contour map of the integrated intensity, $\int T_R dv$, of the ^{12}CO $J=1$–0 emission within the velocity range from $V_{LSR}=-10\,\mathrm{km\,s^{-1}}$ to $-5\,\mathrm{km\,s^{-1}}$. The observed points are also indicated in figure 1 with crosses. Unfortunately, weather conditions were poor while the ^{12}CO data were taken; therefore, we smoothed the original ^{12}CO map to a spatial resolution of 30″ in order to improve the signal-to-noise ratio, obtaining figure 1. However, this map clearly shows a dip of the intensity of ^{12}CO emission near the globule center and a hump between the dip and the eastern edge. The map of the ^{13}CO integrated intensity over the same velocity interval as in figure 1, is displayed in figure 2, and is superposed on a photograph of the globule. It demonstrates that the above-mentioned dip and hump correspond to a real cavity and the ridge of the ^{13}CO column density, respectively, as was suggested by Wootten et al. (1983).

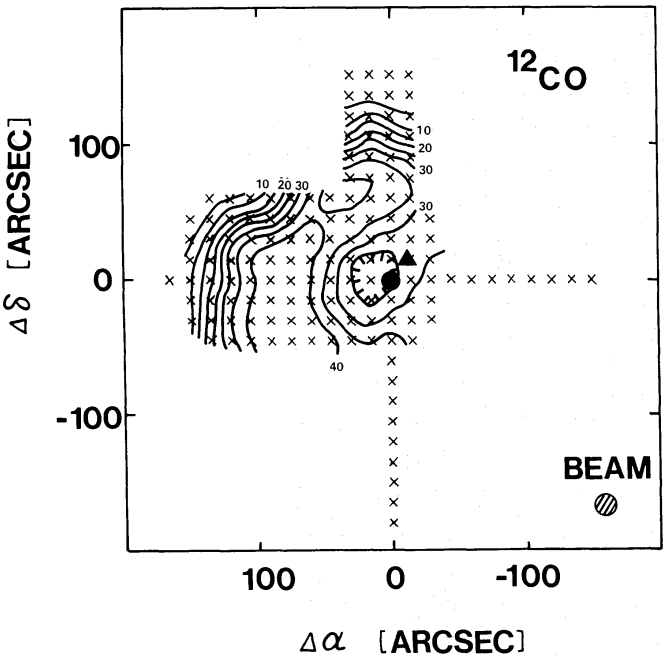

Fig. 1. A contour map of the integrated radiation temperature $I=\int T_R dv$ of ^{12}CO $J=1$–0 emission for the velocity range from -10 to $-5\,\mathrm{km\,s^{-1}}$. Both the lowest contour level and contour interval are $5\,\mathrm{K\,km\,s^{-1}}$. The observed points are indicated by crosses. The positions of LkHα 349 and LkHα 349/c are shown by the filled circle and triangle, respectively. The shadowed circle at the lower-right corner corresponds to the beam size. The offsets are in arcsec with respect to the position of LkHα 349.

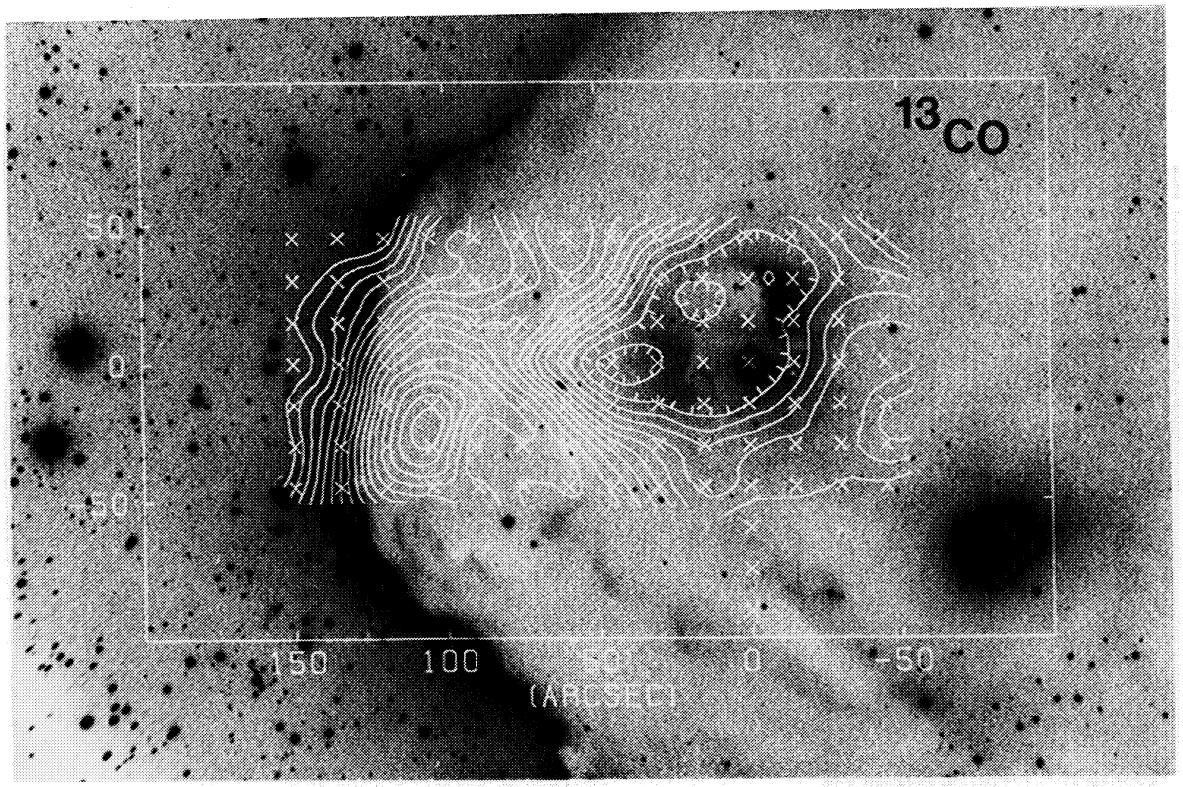

Fig. 2. A map of the central part of the globule, showing the spatial distribution of the integrated intensity $\int T_R dv$ of the ^{13}CO emission, is superposed on a photograph in the red taken with the 200-inch reflector (courtesy of Dr. D. E. Osterbrock). The observed points are indicated by crosses. The velocity range of integration is between -10 and $-5\,km\,s^{-1}$. The lowest contour level and the contour interval is 3.6 and $1.8\,K\,km\,s^{-1}$, respectively.

It appears that the structure of the cavity is well correlated with the feature of optical nebulosities and the distribution of faint stars.

Figures 3a and b are position-velocity maps of ^{12}CO along the east-west and north-south strips through the globule center, respectively. Figure 4 is also a position velocity map of ^{13}CO along the east-west strip. The average line width of ^{12}CO and ^{13}CO is $1.5\,km\,s^{-1}$, and the mean radial velocity is $V_{LSR} = -7.8\,km\,s^{-1}$. Practically no systematic velocity change has been found along both strips. Figures 3a and b show another velocity component at $V_{LSR} = 0\,km\,s^{-1}$. Since there are no intensity and velocity variations of this component through the face of the globule, we interpret it as being due to a foreground cloud The line width of ^{13}CO shows some variation, the average being around $1.5\,km\,s^{-1}$; its radial velocity is about the same as that of ^{12}CO. The radial velocity of the ionized gas of IC 1396 has been observed to be $-2.2\,km\,s^{-1}$ in Hα (Georgelin and Georgelin 1970) and $-1.9\,km\,s^{-1}$ in H166α (Pedlar 1980), which are about $6\,km\,s^{-1}$ greater than the radial velocity of the molecular gas. If the ionized gas is expanding with respect to the molecular gas, this velocity difference may indicate that the globule is located in front of the H II region IC 1396.

3.2. *Optical Spectroscopy*

Our spectrograms of the nebulosity show the emission of Balmer lines as well as

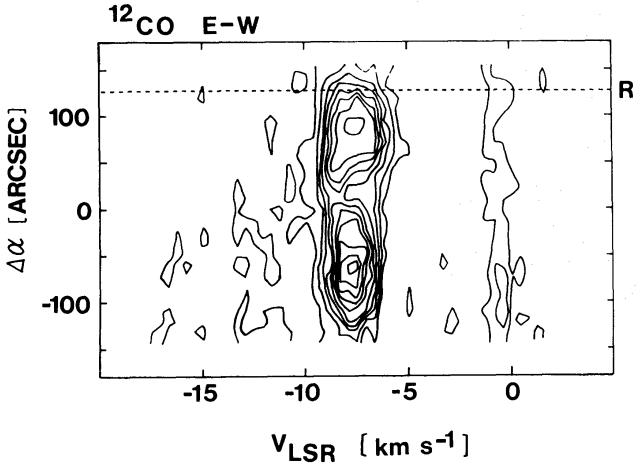

Fig. 3a. The position-velocity map along the EW strip for the ^{12}CO emissions passing the center. The lowest contour level and the contour interval is 1 and 2 K, respectively. The eastern rim is indicated by "R".

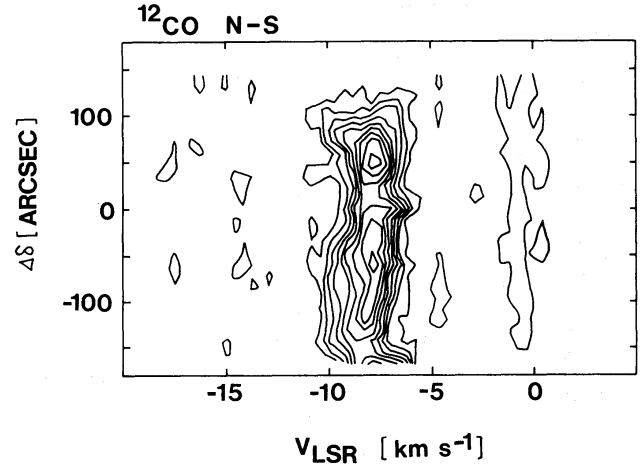

Fig. 3b. Same as figure 3a, but for the NS strip.

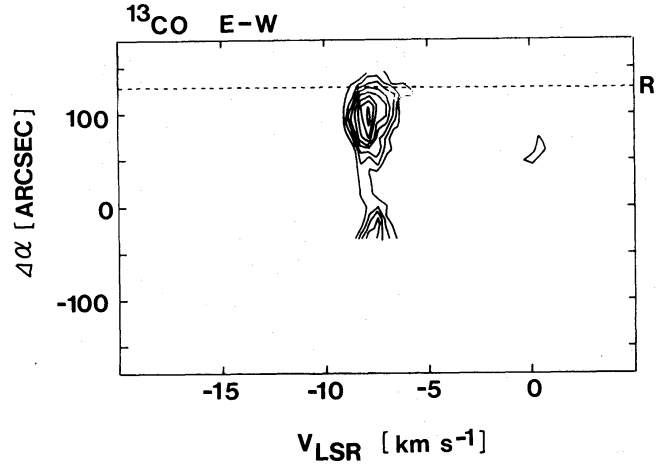

Fig. 4. The position-velocity map along the EW strip for ^{13}CO emissions. Both the lowest contour level and the contour interval are 0.8 K km s^{-1}. The eastern rim is indicated by "R".

of low- and high-excitation forbidden lines, such as [S II] λ6717, 6731, [N II] λ6583, [N I] λ5199, [O III] λ4959, 5007, and [O II] λ3727. There is probably no [O I] λ6300, 6363 emission, though it is difficult to say unambiguously, due to the existence of strong background emission from the night sky. Practically no continuum has been found.

We therefore conclude that the nebulosity is an H II region.

4. Discussion

4.1. Globule

We can estimate the H_2 column densities through the cloud by computing the LTE ^{13}CO column densities from our ^{12}CO and ^{13}CO data. Obtained LTE ^{13}CO column densities were converted to those of H_2 by using Dickman's (1978) ratio $N(H_2)/N(^{13}CO) = 5 \times 10^5$. Figure 5 shows the excitation temperature and the column density plotted as a function of position along the EW strip. The position of the bright rim is indicated.

The density peak lies 0.1 pc inside the bright rim and its extent is about 0.1 pc. This peaking seems to be due to some interaction between the globule and the H II region. The excitation temperature of CO $J=1$–0 emissions was also calculated using the equation for the optically thick limit and the data of Wootten et al. (1983). The result is shown in figure 5, indicating that the excitation temperature of the $J=1$–0 transition decreases toward the cavity center, whereas the $J=2$–1 data (Wootten et al. 1983) give a roughly constant temperature of 25 K throughout the globule.

If we assume that the structure of the globule is a ring of uniform density (seen face-on), the total mass can be estimated. Adopting 45″ (0.16 pc) for the inner radius

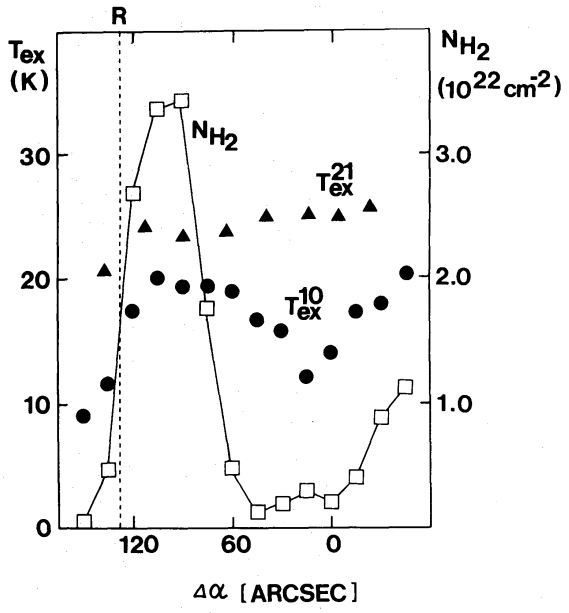

Fig. 5. The column density $N(H_2)$ and the excitation temperatures of $J=1$–0 and $J=2$–1 ^{12}CO transition (T_{ex}^{10}, T_{ex}^{21}) are plotted as a function of position along the EW strip. The offsets are in arcsec with respect to the position of LkHα 349. The rim of the globule is indicated by "R".

of the ring, 110″ (0.4 pc) for the outer radius and 1.5×10^{22} cm^{-2} for the average column density, the total mass of the globule was calculated to be about $120 M_{\odot}$. The virial mass of the globule was estimated as $M_{v} \sim \sigma^2 R/G \sim 0.54 \Delta V^2 R/G = 110 M_{\odot}$, which is comparable to the molecular mass estimated above. This means that the globule is critically stable. The hottest star in Trumpler 37, HD 206267 (O6V), exists 20′ away from the globule. If we assume that the angle between the line of sight and the line connecting the globule and this star is 45°, the separation corresponds to the distance 6 pc. Following Reipurth (1983), we can estimate the time scale of the evaporation of the globule due to the ultra-violet radiation from HD 206267. However, the derived time scale of $\tau_{ev} = 9 \times 10^5$ yr is a lower limit, since the shielding effect by dust is neglected. This may be comparable to the dynamical time scale, $\tau_{dy} \sim R/(\sigma/2) \sim 5 \times 10^5$ yr.

4.2. *Bright Rim*

The bright rim IC 1396A at the eastern edge of the globule has been observed at various wavelengths (Pottasch 1956; Osterbrock 1957; Schmidt 1974; Baars and Wendker 1976; Matthews 1979; Wootten et al. 1983; Schwartz 1985). Here, we pay attention to this portion of figures 3a and 4. $T_R(^{12}CO)$ and $T_R(^{13}CO)$ fall off sharply in 1 arcmin. Such a sharp boundary has been observed in the CS $J = 1$–0 line across the bright bar

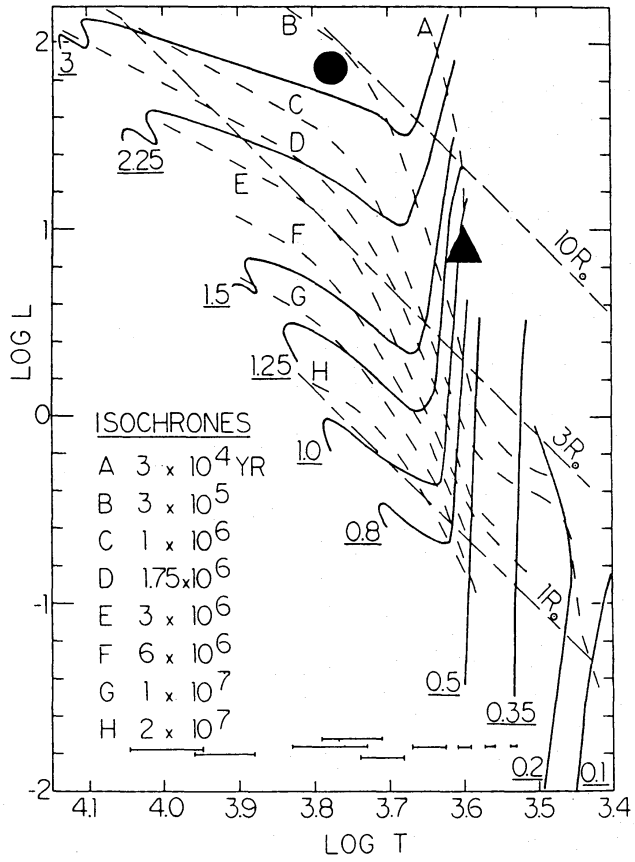

Fig. 6. The positions of LkHα 349 and LkHα 349/c on the theoretical HR diagram with convective-radiative evolutionary tracks, isochrones and lines of constant radius (Cohen and Kuhi 1979).

of the Orion Nebula (Omodaka et al. 1984). Contrary to the case of the Orion bright bar, however, we have failed to detect any velocity variation across the bright rim. This may be due to the difference in the line of sight in the two cases. It seems that we observed IC 1396A from a nearly tangential perspective.

4.3. LkHα 349 and LkHα 349/c

Cohen and Kuhi (1979) gave the spectral type of LkHα 349 and LkHα 349/c as F8 and K7, respectively. Adopting 750 pc for the distance of IC 1396, we found the bolometric luminosities of these stars to be $84L_{\odot}$ and $9L_{\odot}$, respectively, from the data given by the above-mentioned authors. Figure 6 shows their locations in a $\log L$-$\log T_{e}$ diagram together with convective-radiative evolutionary tracks, isochrones and lines of constant radius adopted from Cohen and Kuhi (1979). It was found that both the stars are still in the stage of pre-main sequence with roughly the same ages ($\sim 10^{5}$ yr), suggesting their simultaneous birth.

The two stars could be formed in the globules through an interaction with the expanding H II region. The radiative implosion of such a globule has been proposed to be one of the mechanisms which might trigger stellar birth (LaRosa 1983; Sandford et al. 1984). According to the results of LaRosa (1983), globules of this size can implode and form stars.

We can calculate the visual extinction A_{v} toward the two stars using the relation $A_{v}=2.0\times 10^{-16}N(^{13}\mathrm{CO})$. The result is $A_{v}=2.6$ mag, which is consistent with $A_{v}=3.65$ mag derived from the optical observations of LkHα 349 (Cohen and Kuhi 1979). This means that LkHα 349 lies behind the globule. On the optical photograph (see figure 2) several faint stars can be seen around LkHα349. The number density of these stars is nearly the same as that in the field outside the globule. This supports the idea that the cavity in the distribution of CO intensity is not caused by the photo-dissociation of molecules but, rather, the depletion of material. The good correlation between the nebulosities and the shape of the CO cavity suggests that the nebulosity is part of the ionized gas of IC 1396 seen through the cavity. If we adopt the radius of the cavity as being 0.16 pc, and the expected average column density as $1.5\times 10^{22}\,\mathrm{cm}^{-2}$ (see section 4.1), then the mass of depleted material is estimated to be about $20M_{\odot}$.

4.4. Possible Origin of the Cavity

A cavity structure was recently found around some young stellar objects (YSOs) which show a high-velocity molecular outflow (e.g., Snell and Schloerb 1985; Mathieu et al. 1988); the strong stellar wind from the YSOs is the most likely cause to form such cavities. The scanner spectrum of LkHα 349 given by Cohen and Kuhi (1979) shows a remarkably conspicuous P Cygni profile in the Hα line, indicating a strong stellar wind from the star; however, no trace of such a profile can be seen in LkHα 349/c. In order to investigate the possible molecular outflow associated with LkHα 349 (or LkHα 349/c), we averaged the ^{12}CO spectra for twenty-three points inside a cavity with uniform weight. The result, shown in figure 7, gives no evidence for a high-velocity wing.

The YSOs associated with cavities tend to be bright in the far infrared. However,

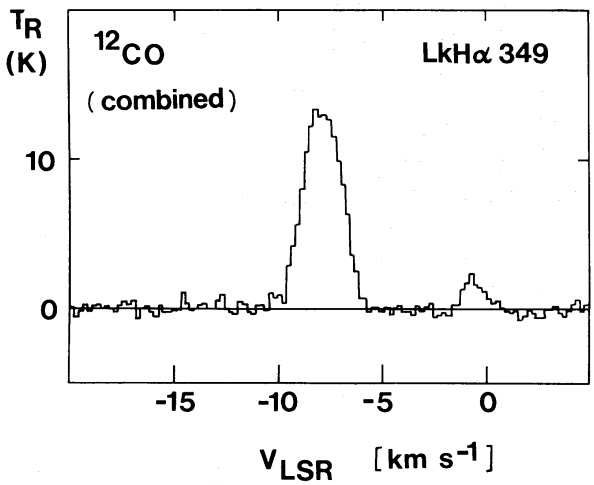

Fig. 7. The combined profile of 23 ^{12}CO line spectra around LkHα 349.

LkHα 349 is not listed in the IRAS point-source catalog. Cantó et al. (1984) observed several Herbig Ae/Be stars in the CO and ^{13}CO line while searching for molecular outflow, and studied the relation between the detectability of the outflow, the parameter r of Cohen and Schwartz (1976) (which is the ratio of the unreddened flux for $\lambda > 0.9\,\mu$m to that for $\lambda < 0.9\,\mu$m) and A_v^{op}/A_v^{CO} (the ratio of the visual extinction determined from the optical spectra to that estimated from the amount of the molecular material along the line of sight). They found that the Herbig Ae/Be stars associated with the outflow phenomena tend to have larger r and A_v^{op}/A_v^{CO}. For LkHα 349 both parameters are small with $r \sim 0.8$ and $A_v^{op}/A_v^{CO} < 1$; hence, outflow is not to be expected. These facts suggest that although LkHα 349 and LkHα 349/c are still in the pre-main sequence stage, they have already passed the active phase to produce an outflow. The cavity we observed might be a hole formed when the outflow was intense.

The authors wish to express their hearty thanks to the staff members of Nobeyama Radio Observatory, and Okayama Astrophysical Observatory for their support during the observations. They are also grateful to Prof. D. E. Osterbrock for providing them with a copy of an inspiring photograph of the globule. This study was supported in part by the Scientific Research Fund of the Ministry of Education, Science, and Culture (63740134). The data processing was carried out on a FACOM-M380 at NRO.

References

Baars, J. W. M., and Wendker, H. J. 1976, *Astron. Astrophys.*, **49**, 473.
Cantó, J., Rodríguez, L. F., Calvet, N., and Levreault, R. M. 1984, *Astrophys. J.*, **282**, 631.
Cohen, M., and Kuhi, L. V. 1979, *Astrophys. J. Suppl.*, **41**, 743.
Cohen, M., and Schwartz, R. D. 1976, *Monthly Notices Roy. Astron. Soc.*, **174**, 137.
Dibai, É. A., and Esipov, V. F. 1968, *Soviet Astron.*, **12**, 448.
Dickman, R. L. 1978, *Astrophys. J. Suppl.*, **37**, 407.
Georgelin, Y. P., and Georgelin, Y. M. 1970, *Astron. Astrophys.*, **6**, 349.
Hayashi, M., Hasegawa, T., Omodaka, T., Hayashi, S. S., and Miyawaki, R. 1987, *Astrophys. J.*, **312**, 327.

Herbig, G. H., and Rao, N. K. 1972, *Astrophys. J.*, **174**, 401.
LaRosa, T. N. 1983, *Astrophys. J.*, **274**, 815.
Loren, R. B., Peters, W. L., and Vanden Bout, P. A. 1975, *Astrophys. J.*, **195**, 75.
Mathieu, R. D., Benson, P. J., Fuller, G. A., Myers, P. C., and Schild, R. E. 1988, *Astrophys. J.*, **330**, 385.
Matthews, H. E. 1979, *Astron. Astrophys.*, **75**, 345.
Omodaka, T., Hayashi, M., and Hasegawa, T. 1984, *Astrophys. J. Letters*, **282**, L77.
Osterbrock, D. E. 1957, *Astrophys. J.*, **125**, 622.
Pedlar, A. 1980, *Monthly Notices Roy. Astron. Soc.*, **192**, 179.
Pottasch, S. 1956, *Bull. Astron. Netherlands*, **13**, 77.
Reipurth, B. 1983, *Astron. Astrophys.*, **117**, 183.
Sandford, M. T., II, Whitaker, R. W., and Klein, R. I. 1984, *Astrophys. J.*, **282**, 178.
Schmidt, E. G. 1974, *Monthly Notices Roy. Astron. Soc.*, **169**, 97.
Schwartz, P. R. 1985, *Astrophys. J.*, **298**, 292.
Snell, R. L., and Schloerb, F. P. 1985, *Astrophys. J.*, **295**, 490.
Wootten, A., Sargent, A., Knapp, G., and Huggins, P. J. 1983, *Astrophys. J.*, **269**, 147.